RSC Advances

PAPER

View Article Online
View Journal | View Issue

Cite this: *RSC Adv.*, 2023, **13**, 2884

Pyrazolone-type compounds (part II): *in vitro* and *in silico* evaluation of antioxidant potential; structure–activity relationship†

Jovica Branković, [a] Vesna M. Milovanović, [b] Zorica D. Petrović, [a] Dušica Simijonović [c] and Vladimir P. Petrović *[a]

The pyrazolone class comprises a variety of hybrid compounds displaying diverse biological actions. Although studied for decades, these compounds are still of interest due to their facile chemical transformations. In our previous work, we presented the synthetic route of functionalised pyrazolone derivatives. The presence of pyrazolone structural motif in many drugs, such as edaravone, prompted us to investigate the antioxidant features of the selected compounds. In this paper, we provide an extensive *in vitro* and *in silico* description of the antioxidant properties of selected pyrazolone analogues. The obtained *in vitro* results revealed their great antiradical potency against the DPPH radical (IC_{50} values in the 2.6–7.8 μM range), where the best results were obtained for analogues bearing a catechol moiety. Density functional theory (DFT) was used to assess their antioxidant capacity from the thermodynamic aspect. Here, good agreement with *in vitro* results was achieved. DFT was employed for the prediction of the most preferable radical scavenging pathway, also. In polar solvents, the SPLET mechanism is a favourable scavenging route, whereas in nonpolar solvents the HAT is slightly predominant. Furthermore, antioxidant mechanisms were studied in the presence of relevant reactive oxygen species. The obtained values of the reaction enthalpies with the selected radicals revealed that HAT is slightly prevailing in polar solvents, while the SPLET mechanism is dominant in nonpolar solvents. Regarding the well-known antioxidant features of the drug edaravone, these findings represent valuable data for this pyrazolone class and could be used as the basis for further investigations.

Received 28th December 2022
Accepted 12th January 2023

DOI: 10.1039/d2ra08280b

rsc.li/rsc-advances

Introduction

Biological exploration of pyrazolone-endowed compounds has continued for more than a century. Ever since its introduction by Ludwig Knorr in 1883,[1] the pyrazolone nucleus evolved into one of the most studied pharmacophores in medicinal chemistry.[2] Such fruitful investigations uncovered diverse biological and therapeutical traits of pyrazolone-based compounds, where a number of them found multiple pharmaceutical roles (Fig. 1).[3,4] Antipyrine (also known as phenazone) as one of the first synthetic drugs, alongside salicylate derivatives, *i.e.*, aspirin, revolutionised the era of antipyretics and fever suppressants.[5] Furthermore, the ampyrone sulfonate family representative, the drug metamizole, is a well-known pain reliever used in various acute/chronic conditions.[6] Also, the pyrazolone skeleton is frequently embedded in many drugs (and drug candidates) for the treatment of various illnesses, such as eltrombopag, piperylone, nifenazone, morazone, propyphenazone, aminophenazone, *etc* (Fig. 1).[4] Such an outcome was triggered by the diversity of pyrazolone-based compounds and their richness in beneficial biological virtues.[2,7] Pyrazolone-cored derivatives mostly wield antimicrobial,[8–13] anticancer,[7,12,14,15] antiproliferative,[14,16] and antiinflammatory potency,[17–22] but they were also identified as analgesics,[18,22,23] antivirals,[24–26] hypoglycaemics,[27] and antioxidants.[11,28,29] The utilisation of pyrazolone synthon produced numerous hybrid molecules acting as multitarget agents.[11,12,17,22,30,31] Biomodelling of pyrazolone structural unit emerged compounds with inhibitory activity on many enzymes as well, such as acetylcholinesterase (AChE) and butyrylcholinesterase (BuChE),[30,32] α-amylase,[33] α-glucosidase,[34] cyclooxygenases (COXs),[17,19,21,28,35] HIV-1 integrase,[36] and even towards human telomerase.[37] These accomplishments have enabled pyrazolone-type compounds to be considered in the treatment of complex illnesses, particularly in neurodegenerative diseases (NDDs), such as Alzheimer's and Parkinson's.[30,32,38] Here, it is important to reference the FDA-approved pyrazolone drug edaravone.[39]

[a]*University of Kragujevac, Faculty of Science, Department of Chemistry, R. Domanovića 12, 34000 Kragujevac, Serbia. E-mail: vladimir.petrovic@pmf.kg.ac.rs*

[b]*University of Kragujevac, Faculty of Agronomy, Department of Chemistry and Chemical Engineering, Cara Dušana 34, 32000 Čačak, Serbia*

[c]*University of Kragujevac, Institute for Information Technologies, Department of Science, Jovana Cvijića bb, 34000 Kragujevac, Serbia*

† Electronic supplementary information (ESI) available. See DOI: https://doi.org/10.1039/d2ra08280b

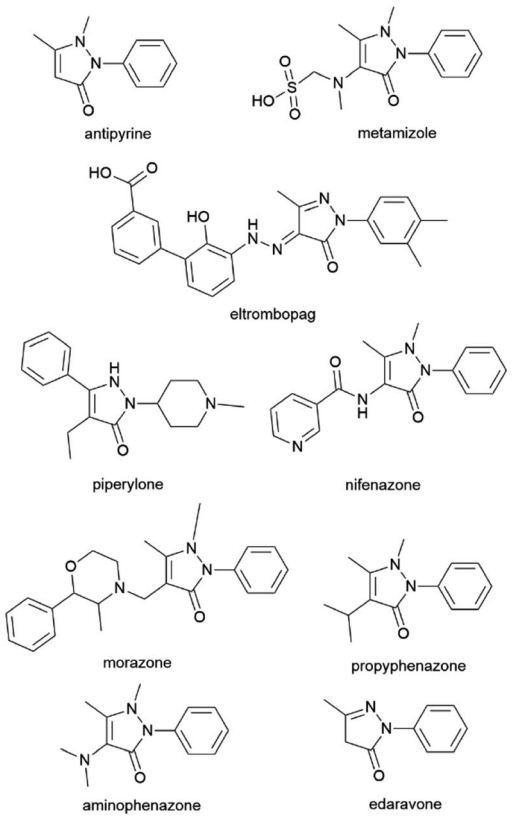

Fig. 1 Drugs containing pyrazolone structural fragment.

This drug is used in the treatment of acute cerebral infarction and has also exhibited a neuroprotective effect in amyotrophic lateral sclerosis (ALS) and Parkinson's disease.[40] Edaravone is designated as a specific chemical entity, empowered for synthetic modifications and diverse usages.[39] It was found that edaravone expresses preventive action in myocardial injury following ischemia and myocardial infarction,[27] and it can be used in chronic obstructive pulmonary disease (COPD), Alzheimer's, rheumatoid arthritis, the treatment of cancer therapy side effects, and many other conditions.[39] Such multipurpose potential of edaravone, particularly its role as a neuroprotective agent, is possible due to its antioxidant ability. Namely, edaravone acts as a potent free radical scavenger that prevents oxidative damage to the cell membrane, *i.e.*, peroxidation of the cell membrane's fatty acids, and therefore, neuronal death and brain edema.[2] The overproduction of free radicals leading to oxidative stress is designated as one of the leading causes of brain ischemic injury.[41,42] Regarding this, the beneficial action of edaravone lies in its ability to quench $^{\bullet}OH$ radicals, as well as other harmful reactive oxygen/nitrogen radical species (ROS and RNS).[43]

Although studied for decades, all these findings indicate the enormous potential of the pyrazolone entity and its almost "never-ending" exploitation in the field of medicinal chemistry. The development of novel edaravone-like and other functionalised pyrazolone scaffolds is still encouraged, as it's recognised as the essence of pharmacological and combinatorial chemistry.[2]

Herein, the versatility of pyrazolone-derived compounds, as well as the multifunctionality of the drug edaravone, inspired us to investigate the antioxidant potential of differently functionalised pyrazolone derivatives, using both *in vitro* and *in silico* methods. In our previous work, we reported the synthetic route for twenty pyrazolone analogues and investigated their potential antiviral activity against the SARS-CoV-2 virus.[44] Generally, the biological investigations on these particular pyrazolone-type derivatives are scarce, *i.e.*, the research is mainly focused on the development of novel synthetic procedures.[45–52] To our knowledge, only one paper reported *in vitro* studies related to these compounds.[53] Bearing this in mind, in this work, we have provided an extensive description of the antioxidant properties of the selected pyrazolone compounds. The insight into their radical scavenging features represents valuable data for this class of pyrazolones and could indicate the compounds with the prospect of neuroprotective application.

Results and discussion

Antioxidant activity of compounds a–t against DPPH radical

In our previous report,[44] twenty pyrazolone derivatives **a–t** bearing different ring C substitution were synthesised and characterised (Table 1). The crystal structure analysis of compound **p** revealed the differences between rings A and B, *i.e.*, the existence of pyrazolone and pyrazole moiety.[44] In this work, compounds **a–t** were subjected to *in vitro* antioxidant screening using the 2,2-diphenyl-1-picrylhydrazyl (DPPH) assay (Table 2). This method was selected since it is noted as reliable for the prediction of the radical scavenging activity against reactive oxygen species present in the living cell.[54,55] The structures of the investigated compounds **a–t** bearing different ring C substitution are presented in Table 1. Here, compound **a** represents a non-substituted analogue. Furthermore,

Table 1 Structural characteristics and ring C substitution of compounds **a–t**

Entry	R^1	R^2	R^3	R^4	Skeleton of compounds **a–t**
a	H	H	H	H	
b	OH	H	H	H	
c	H	OH	H	H	
d	H	H	OH	H	
e	H	Cl	H	H	
f	H	H	Cl	H	
g	H	H	F	H	
h	NO_2	H	H	H	
i	H	NO_2	H	H	
j	H	H	NO_2	H	
k	CH_3	H	H	H	
l	H	CH_3	H	H	
m	OH	OH	H	H	
n	H	OH	OH	H	
o	OH	OCH_3	H	H	
p	H	OCH_3	OH	H	
q	H	OCH_3	OH	OCH_3	
r	H	OH	OCH_3	OCH_3	
s	H	OCH_3	OCH_3	OCH_3	
t	OH	Cl	H	Cl	

Table 2 *In vitro* interactions of selected compounds **a–t** with DPPH radical

Inhibition (%)								
Concentration (μM)	100		50		25			
Compound	20 min	60 min	20 min	60 min	20 min	60 min	IC_{50} (μM)	SF
a	96.1 ± 1.1	97.4 ± 0.2	95.8 ± 0.4	96.6 ± 0.6	93.6 ± 0.4	94.4 ± 0.8	5.1 ± 0.1	2.5
b	91.6 ± 0.7	93.2 ± 1.5	91.5 ± 1.3	92.1 ± 2.2	86.9 ± 4.7	89.8 ± 4.6	6.2 ± 0.1	2.0
c	94.9 ± 0.1	95.4 ± 0.1	94.2 ± 0.2	95.3 ± 0.2	91.9 ± 0.7	93.9 ± 0.6	4.3 ± 0.1	2.9
d	95.7 ± 1.1	95.8 ± 0.5	95.1 ± 0.7	95.4 ± 0.3	93.1 ± 0.9	94.3 ± 1.0	4.9 ± 0.1	2.6
e	93.3 ± 2.1	94.4 ± 1.3	93.1 ± 1.9	94.3 ± 0.8	89.8 ± 0.5	93.8 ± 2.2	4.5 ± 0.1	2.8
f	95.8 ± 0.2	95.9 ± 0.2	93.4 ± 0.2	95.3 ± 0.5	92.2 ± 0.7	94.3 ± 0.2	5.4 ± 0.1	2.3
g	93.4 ± 1.3	94.7 ± 0.1	92.8 ± 1.0	93.9 ± 1.0	90.2 ± 0.3	92.6 ± 0.8	4.8 ± 0.1	2.6
h	95.6 ± 0.2	97.2 ± 0.6	87.9 ± 0.7	92.1 ± 0.3	80.5 ± 0.7	88.8 ± 0.6	7.8 ± 0.1	1.6
i	95.7 ± 0.1	95.8 ± 0.1	92.4 ± 1.0	94.3 ± 0.4	92.1 ± 0.8	94.2 ± 0.5	4.5 ± 0.1	2.8
j	95.1 ± 0.7	95.3 ± 0.1	92.1 ± 1.1	93.1 ± 1.1	85.1 ± 0.9	89.2 ± 0.2	5.1 ± 0.1	2.5
k	96.3 ± 1.0	98.3 ± 0.7	96.2 ± 0.2	96.3 ± 0.4	94.6 ± 0.6	96.2 ± 0.8	4.2 ± 0.1	3.0
l	95.0 ± 0.6	95.1 ± 0.5	94.9 ± 0.5	95.0 ± 0.6	92.2 ± 1.1	93.8 ± 0.8	3.5 ± 0.1	3.6
m	96.7 ± 0.3	97.2 ± 0.2	95.8 ± 0.2	96.4 ± 0.3	94.4 ± 0.6	94.9 ± 0.8	2.6 ± 0.1	4.8
n	94.9 ± 0.3	96.7 ± 0.3	94.3 ± 1.6	94.9 ± 0.3	94.2 ± 0.9	94.3 ± 1.1	2.9 ± 0.1	4.3
o	91.6 ± 1.1	91.7 ± 0.1	89.7 ± 0.7	90.4 ± 0.7	89.4 ± 0.9	89.6 ± 1.6	3.6 ± 0.1	3.5
p	93.6 ± 0.2	94.5 ± 0.2	92.3 ± 0.4	93.2 ± 1.3	91.7 ± 0.6	92.0 ± 0.6	6.1 ± 0.1	2.0
q	92.1 ± 0.4	93.9 ± 1.2	90.9 ± 0.8	91.7 ± 0.2	89.9 ± 0.6	90.7 ± 0.7	5.5 ± 0.1	2.3
r	95.1 ± 0.6	95.2 ± 0.1	94.4 ± 0.3	94.9 ± 0.9	90.5 ± 0.1	94.7 ± 0.2	4.4 ± 0.1	2.8
s	96.1 ± 0.1	96.8 ± 0.2	94.2 ± 0.8	94.8 ± 0.6	89.8 ± 1.1	92.8 ± 1.1	6.2 ± 0.1	2.0
t	88.5 ± 0.5	89.8 ± 0.7	88.1 ± 0.9	89.6 ± 0.7	84.2 ± 1.0	89.6 ± 0.9	6.4 ± 0.1	2.0
Pyrazolone	93.7 ± 0.1	95.5 ± 0.8	92.8 ± 1.2	94.5 ± 0.8	86.9 ± 1.6	92.3 ± 0.8	9.3 ± 0.1	1.3
NDGA	94.5 ± 0.2	94.1 ± 0.7	94.2 ± 0.7	94.2 ± 0.7	94.6 ± 0.7	94.6 ± 0.6	1.7 ± 0.1	7.4
Quercetin	95.1 ± 0.9	95.4 ± 0.8	96.8 ± 1.0	96.5 ± 0.9	95.3 ± 0.8	95.1 ± 0.9	1.9 ± 0.1	6.6

derivatives **b**, **c**, and **d** possess one –OH group in R^1, R^2, and R^3 positions (respectively). Analogues **e**, **f**, and **g** bear one halogen atom (chlorine or fluor), whereas **h**, **i**, and **j** carry the nitro group in different positions.

Methyl groups are introduced to the C ring in the case of compounds **k** and **l**, whereas derivatives **m–s** possess multiple –OH and/or $–OCH_3$ groups. Finally, compound **t** bear R^1–OH group on ring C, as well as two chlorine atoms.

Based on the obtained results, all analogues exhibited antioxidant activity against DPPH radical with IC_{50} values in the range of 2.6–7.8 μM. It is worth emphasizing that the parent pyrazolone compound (5-methyl-2,4-dihydro-3*H*-pyrazol-3-one) was also tested against the DPPH radical, with the expectation of enhanced antioxidant activity of compounds **a–t**. Based on the obtained results, all compounds expressed higher antiradical activity in comparison to their parent compound (Table 2). Furthermore, the antioxidant capacity of the investigated compounds was expressed through the values of stoichiometric factor (SF). Namely, if the value of SF is ≥2, such compound is designated as a good antioxidant. The results presented in Table 2 indicate that all compounds, except **h** (SF = 1.6), could be noted as good antioxidants (SF values in the range of 2.0–4.8). The obtained results could be compared to other findings, *i.e.*, with compounds bearing pyrazolone fragment.[27,56–60] Here, in comparison with the most similar edaravone-like set of compounds (and drug edaravone),[27] compounds **a–t** expressed significantly higher antioxidant activity.

The ring C substitution effect on antioxidant activity. Besides the aim to investigate the antioxidant properties of compounds **a–t**, one of the objectives was to evaluate how the ring C substitution impacts the inhibition potency of the DPPH radical. Here, the non-substituted analogue **a** expressed good activity against DPPH ($IC_{50} = 5.1 \pm 0.1$ μM). In comparison to **a**, among those bearing only one –OH group, the best result was obtained for derivative **c** (R^2–OH; $IC_{50} = 4.3 \pm 0.1$ μM). These results, *i.e.*, the more favourable R^2–substitution over R^1– and R^3–, are in agreement with literature data obtained for compounds with a similar set of rings.[27] In the cases of halogen-substituted C ring, compounds **e** (R^2–Cl) and **g** (R^3–F) exhibited higher activity than **a**, whereas **f** (R^3–Cl) was slightly lower. Here, the best activity expressed derivative **e** ($IC_{50} = 4.5 \pm 0.1$ μM). Among those bearing nitro group, the R^2–substituted derivative **i** expressed the highest inhibition activity compared to **a** ($IC_{50} = 4.5 \pm 0.1$ μM), whereas the R^1–substituted **h** the lowest ($IC_{50} = 7.8 \pm 0.1$ μM). Such findings are in agreement with the literature data, also.[27] Similarly, for compounds **k** and **l**, the best interaction with DPPH was achieved in the case of R^2–CH_3 substituted analogue **l** ($IC_{50} = 3.5 \pm 0.1$ μM). For compounds **m–s**, the highest inhibition activity against the DPPH radical expressed analogue **m** (R^1, R^2–diOH), which was also the best result achieved among all tested compounds ($IC_{50} = 2.6 \pm 0.1$ μM). It is worth emphasizing that analogues **n**, **o**, and **r** also exhibited noteworthy antioxidant activity ($IC_{50} = 2.9 \pm 0.1$, 3.6 ± 0.1, and 4.4 ± 0.1 μM, respectively). Here, it is important to point out that derivatives **n** and **r** possess the R^2–OH group,

whereas compound **o** bears *o*-vanillin moiety. Finally, the antioxidant activity of derivative **t** was lower compared to compound **a**, *i.e.*, similar to the activity of compound **b**. Here, both **b** and **t** possess R^1–OH group, whereas **t** bear additional two chlorine atoms.

Based on the obtained results, several remarks could be noted:

(1) All compounds expressed higher inhibition activity than the parent pyrazolone compound, and FDA-drug edaravone ($IC_{50} = 18.1 \pm 0.5$)[27] as well;

(2) Ring C substitution, *i.e.*, number, nature, and the position of specific groups, alters the antioxidant potency of the investigated compounds toward DPPH radical;

(3) The R^2–substitution most significantly enhances the antioxidant activity in comparison to the other positions, as well as to non-substituted derivative **a**. This can easily be observed in the cases of derivatives **c** (R^2–OH), **e** (R^2–Cl), **i** (R^2–NO_2), and **l** (R^2–CH_3); the antioxidant activity is even more heightened when an additional group is neighbouring the R^2–substituent. Such observations were made for the compounds **m**, **n**, **o**, and **r** which bear the –OH and neighbouring –OH or –OCH_3 groups. This can be attributed to the formation of corresponding phenolic O˙ radical which is stabilised through resonance and electron-donating effects of the neighbouring group.[61] Moreover, in the cases of compounds **m** and **n**, even better stabilisation can be achieved *via* intramolecular hydrogen bonding between the O˙ radical and the neighbouring –OH group, which is unique for catechol-like compounds.[62–64] These statements are in the agreement with the obtained IC_{50} values for these derivatives;

(4) Besides the substituent position, the nature of the particular group is also influencing the antioxidant activity. This can be observed in the cases of compounds **b** (R^1–OH), **h** (R^1–NO_2), and **k** (R^1–CH_3), where the groups with different electronic properties (electron-donating/withdrawal) are present. The results obtained for compound **k** suggest enhanced antioxidant activity if the R^1-substituent possesses an electron-donating effect (such as the –CH_3 group). In this respect, it is shown that the group in the R^1–position with a strong electron-withdrawal effect (such as –NO_2) is not favourable. Generally, the R^1–substitution is the least favourable for antioxidant activity compared to R^2– and R^3–. However, by comparing the results obtained for R^1–substituted compounds **b**, **m**, **o**, and **t** (R^1–OH group), it was observed that the presence of an additional neighbouring group with an electron-donating effect improves antioxidant activity (compound **m** and **o**), whereas the presence of halogen groups has almost no effect (compound **t**). On the other hand, in the cases of R^2–substituted derivatives **c** (R^2–OH), **e** (R^2–Cl), and **i** (R^2–NO_2), similar values of IC_{50} were obtained, which suggests that, in this position, the electronic properties of the particular group are not noticeably influencing the antioxidant activity. The slight exception to this trend is compound **l** (R^2–CH_3), which expressed somewhat higher activity than **c**, **e**, and **i**.

(5) Finally, the number of present groups also influences the antioxidant activity but is dependent on their position and nature. Here, compounds **p** (bearing vanillin moiety), **q** (possessing syringaldehyde fragment), and **s** (having three methoxy groups) can be compared. All three compounds expressed even lower activity than non-substituted derivative **a**. For derivatives **p** and **s**, similar results were obtained, whereas slightly higher activity was observed for derivative **q**. Such activity of analogue **q** can be appointed to the presence of the –OH group between two methoxy groups, resulting in the better stabilisation of the phenoxy radical. Also, the influence of the position of the –OH group could be observed in cases of **q** (R^3–OH) and **r** (R^2–OH), where **r** expressed higher activity. In this case, it was expected the opposite outcome since the –OH in **q** is neighboured by two –OCH_3 groups. Similarly, analogue **p** should have expressed higher activity than **d**. Nevertheless, some authors suggest that the presence of an additional methoxy group might manifest a negative impact *via* steric effect.[65]

HOMO and LUMO

Energy values of the highest occupied molecular orbital (HOMO) and the lowest unoccupied molecular orbital (LUMO) could be used for the general description of molecule reactivity, in our case, towards DPPH radical. For instance, a higher value of HOMO is indicating a better electron-donating ability of the molecule, which is an important feature for radical scavenging.[66] On the other hand, the energy difference between HOMO and LUMO (HOMO–LUMO gap) is distinguishing the reaction prospect, *i.e.*, the lower the energy gap, the reaction is more likely to happen, while the higher gap indicates higher molecule stability. The results for compounds **a–t** obtained in methanol, water, and benzene are presented in Table 3. Here, small but noticeable differences were observed. The highest energy values of HOMOs were calculated for compounds **m–q**. These findings are in good agreement with experimental results since **m**, **n**, and **o** expressed excellent antioxidant activity against DPPH. On the other hand, the HOMO values of other derivatives were quite similar (−0.224 to −0.227 range), where the lowest correspond to the nitro-substituted derivatives. Here, moderate agreement with the experimental results was achieved, particularly for the analogue **h** which expressed the lowest experimental radical scavenging activity among all tested compounds. Similar trends were obtained in all investigated solvents.

The lowest HOMO–LUMO gaps were calculated for **h**, **i**, and **j**, which evidently deviate from the values obtained for other compounds. Such results were the consequence of their multiple times lower LUMO values in comparison to all other compounds. Although these results for **h**, **i**, and **j**, indicate their enhanced reaction probability with the DPPH radical, the parameters were not distinguished enough to explain their different experimental IC_{50} values. This outcome is suggesting that the activity of **h**, **i**, and **j** is not directly/only linked with the molecule reactivity, *i.e.*, the driving force of the reaction may depend on other factors. On the other hand, if we exclude the results obtained for **h**, **i**, and **j**, a moderate agreement was achieved with the experimental results for other compounds. However, the results are implying the involvement of other

Table 3 Calculated energy values of HOMO and LUMO (eV) in methanol, water, and benzene for compounds **a–t**

	HOMO (eV)			LUMO (eV)			HOMO–LUMO gap (eV)		
Compound	Methanol	Water	Benzene	Methanol	Water	Benzene	Methanol	Water	Benzene
a	−0.226	−0.226	−0.217	−0.026	−0.026	−0.035	0.200	0.200	0.182
b	−0.224	−0.225	−0.214	−0.026	−0.026	−0.031	0.198	0.198	0.183
c	−0.226	−0.226	−0.216	−0.025	−0.026	−0.034	0.200	0.200	0.182
d	−0.225	−0.226	−0.217	−0.027	−0.026	−0.034	0.198	0.199	0.183
e	−0.226	−0.227	−0.220	−0.028	−0.028	−0.037	0.198	0.199	0.183
f	−0.226	−0.227	−0.220	−0.029	−0.029	−0.038	0.196	0.198	0.183
g	−0.225	−0.226	−0.219	−0.029	−0.028	−0.037	0.197	0.198	0.183
h	−0.226	−0.228	−0.220	−0.106	−0.107	−0.100	0.120	0.120	0.121
i	−0.227	−0.228	−0.224	−0.113	−0.114	−0.102	0.115	0.114	0.122
j	−0.227	−0.228	−0.224	−0.112	−0.113	−0.100	0.115	0.115	0.125
k	−0.227	−0.228	−0.220	−0.024	−0.025	−0.034	0.203	0.203	0.187
l	−0.225	−0.226	−0.217	−0.026	−0.026	−0.034	0.199	0.200	0.183
m	−0.222	−0.223	−0.214	−0.024	−0.025	−0.032	0.198	0.198	0.182
n	−0.219	−0.220	−0.215	−0.025	−0.026	−0.034	0.194	0.195	0.181
o	−0.219	−0.220	−0.212	−0.024	−0.024	−0.029	0.195	0.196	0.184
p	−0.216	−0.217	−0.210	−0.025	−0.025	−0.034	0.192	0.192	0.176
q	−0.213	−0.214	−0.203	−0.025	−0.025	−0.035	0.187	0.189	0.168
r	−0.226	−0.227	−0.219	−0.025	−0.026	−0.034	0.201	0.201	0.185
s	−0.225	−0.226	−0.215	−0.026	−0.026	−0.035	0.199	0.200	0.180
t	−0.225	−0.227	−0.219	−0.037	−0.037	−0.041	0.188	0.191	0.178

factors responsible for the interaction of compounds **a–t** with the DPPH radical.

Stabilisation energies (ΔE_{iso})

Stabilisation energies (ΔE_{iso}) were calculated for all investigated compounds to evaluate the radical stability (O$^{\bullet}$ and N$^{\bullet}$) at specified positions (Fig. 2). The results obtained in methanol are presented in Table 4, whereas those in water and benzene are provided in the ESI (Tables S1 and S2†). Here, on pyrazolone ring (A), the formation of two N–radicals was observed (positions N1A and N2A), whereas on pyrazole ring (B) the stabilities of O$^{\bullet}$ and N$^{\bullet}$ radicals were studied (positions O1B and N2B). Depending on the substitution of the phenyl moiety (ring C), corresponding O–radicals were examined (positions O1C, O2C, and O3C). Based on the obtained results in methanol, the lowest ΔE_{iso} values were calculated for the ring C radicals of compounds **m–q** (Table 4). These findings indicate the great involvement of the ring C –OH groups in the antioxidant activity, particularly in the cases **m**, **n**, and **q**, which is in good agreement with experimental results. Similarly, regarding the calculated ΔE_{iso} values, it was observed that ring A also empowers the antioxidant capability of the investigated compounds, whereas the involvement of ring B could be

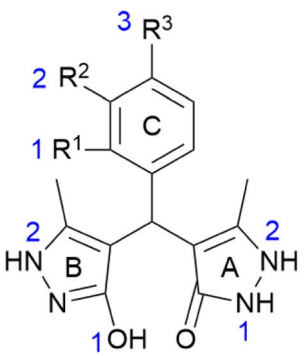

Fig. 2 Positions and labels of the investigated radical species (O$^{\bullet}$ and N$^{\bullet}$). A stand for pyrazolone, B for pyrazole, and C for phenyl ring. The specific positions of the radicals are marked separately for each ring (blue numbers).

Table 4 Calculated stabilisation energies (kJ mol^{-1}) for compounds **a–t** in methanol

	Ring A		Ring B		Ring C		
Entry	N1	N2	O1	N2	O1	O2	O3
a	−5.83	−20.47	−0.58	28.53	—	—	—
b	−5.10	−21.09	−3.55	25.12	−7.99	—	—
c	−5.74	−20.66	0.30	28.75	—	−2.47	—
d	−5.60	−20.20	0.34	29.33	—	—	−9.61
e	−5.03	−19.13	0.07	29.21	—	—	—
f	−4.74	−19.00	0.69	29.76	—	—	—
g	−5.06	−19.44	0.38	29.52	—	—	—
h	−2.31	−15.80	−2.21	31.26	—	—	—
i	−1.95	−15.76	3.90	32.38	—	—	—
j	−3.72	−17.51	0.97	30.99	—	—	—
k	−10.16	−19.18	−5.72	31.59	—	—	—
l	−8.19	−20.66	0.45	28.51	—	—	—
m	−3.79	−18.24	−4.22	29.84	−34.66	−31.42	—
n	−5.04	−19.62	0.20	28.49	—	−33.09	−35.89
o	−4.64	−19.54	−3.04	28.45	−25.59	—	—
p	−6.25	−20.90	0.57	27.74	—	—	−28.48
q	−5.21	−19.93	0.93	29.02	—	—	−44.34
r	−5.41	−19.58	0.82	28.85	—	−17.06	—
s	−5.04	−19.82	1.20	28.90	—	—	—
t	−3.10	−18.05	−1.88	29.76	−12.84	—	—

considered negligible. In this respect, the –NH groups at position 2 of ring A participate significantly in the radical scavenging, whereas a minor contribution of the N1 was noted. In the case of ring B, high energy values suggest insufficient stabilisation of N2 radicals, and thus, no involvement of those –NH groups in the radical scavenging. The results obtained for ring B –OH groups (O1B position) indicated their insignificant contribution to the antioxidant activity, but they, mutually compared, diverse the most. Generally, the obtained results differentiate depending on the present substituents on the ring C. In comparison to the results obtained for **a**, it was observed that a particular substituent differently alters radical stabilisation at a different position. In this respect, considerably better stabilisation of ring N1A radical was noted for analogues **k** and **l**, bearing R^1– and R^2–CH_3, respectively. Also, the stability of the O1B radical is most improved in the case of compound **k**. These statements are in the agreement with their experimental results, *i.e.*, their enhanced activity against DPPH. On the other hand, the N1A is substantially less stable (compared to the non-substituted analogue **a**) if the –NO_2 group is introduced to the ring C (compounds **h**, **i**, and **j**). This effect was also noticed for the N2A radical. Here, the results suggest that nitro-substitution is not favourable. However, compound **i** expressed slightly higher antioxidant activity toward DPPH. Nevertheless, literature reports variations between *in silico* and *in vitro* results regarding the influence of the particular group on radical scavenging.[65] Interestingly, even in the case of the most active compounds **m** and **n**, N1A and N2A radicals are slightly less stable than those in the case of **a**. Still, in such a case, it is clear that the presence of catechol moiety on ring C could overcompensate these minor downsides since the best stabilisation was observed for these radicals.

The results obtained in water were similar to those in methanol, with some exceptions (Table S1†). Generally, the radical stabilisation is somewhat better in water since most values were slightly lower. Excellent agreement for the analogues **b**, **c**, and **d** was achieved. Nitro-substitution was the least favourable, particularly ortho analogue (compound **h**), which corresponds to the obtained experimental results. Moreover, the parameters obtained for compounds **h**, **i**, and **j** were mutually well distinguished. On the other hand, slightly lower stability of the N1A and N2A radicals was observed for compounds **k**, **l**, and **m**. In benzene as a solvent (Table S2†), parameters calculated for the most efficient radical scavengers **l**, **m**, **n**, and **o** were in good accordance with experimental results, as well as for –OH monosubstituted analogues **b**, **c**, and **d**. As in all previous solvents, nitro-substitution was, once again, designated as thermodynamically the least favourable.

Antioxidant mechanism analysis

The estimation of the most preferable radical scavenging pathway for compounds **a–t** was performed by mutual comparison of calculated thermodynamic parameters: bond dissociation enthalpy (BDE), ionisation potential (IP), proton affinity (PA), proton dissociation enthalpy (PDE), and electron transfer enthalpy (ETE). The results obtained in methanol are presented in Tables 5–7, while the others are presented in Tables S3–S8.† Here, several plausible antioxidant mechanisms were considered: hydrogen atom transfer (HAT), single electron transfer-proton transfer (SET-PT), and sequential proton loss electron transfer (SPLET).[67] Namely, all these scavenging pathways lead to the inactivation of radical species, followed by the formation of corresponding radical from the antioxidant. The

Table 5 Calculated bond dissociation enthalpies (kJ mol^{-1}) for compounds **a–t** in methanol

	Bond dissociation enthalpy (BDE) kJ mol^{-1}						
	N1 (A)	N2 (A)	O1 (B)	N2 (B)	O1 (C)	O2 (C)	O3 (C)
a	347	332	352	381	—	—	—
b	347	331	349	378	344	—	—
c	347	332	353	381	—	350	—
d	347	332	353	382	—	—	343
e	347	333	352	382	—	—	—
f	348	333	353	382	—	—	—
g	347	333	353	382	—	—	—
h	350	337	350	384	—	—	—
i	350	337	356	385	—	—	—
j	349	335	353	383	—	—	—
k	342	333	347	384	—	—	—
l	344	332	353	381	—	—	—
m	349	334	348	382	318	321	—
n	347	333	353	381	—	319	317
o	348	333	349	381	327	—	—
p	346	332	353	380	—	—	324
q	347	333	353	381	—	—	308
r	347	333	353	381	—	335	—
s	347	333	354	381	—	—	—
t	349	334	351	382	340	—	—

Table 6 Calculated IP and PDE values (kJ mol^{-1}) for compounds **a–t** in methanol

		PDE						
	IP	N1 (A)	N2 (A)	O1 (B)	N2 (B)	O1 (C)	O2 (C)	O3 (C)
a	457	51	36	56	85	—	—	—
b	456	53	37	54	83	50	—	—
c	458	50	35	56	85	—	54	—
d	466	43	28	49	78	—	—	39
e	460	49	35	54	83	—	—	—
f	460	49	35	55	84	—	—	—
g	459	50	35	55	84	—	—	—
h	463	49	36	49	83	—	—	—
i	465	47	34	53	82	—	—	—
j	464	46	33	51	81	—	—	—
k	457	47	38	51	88	—	—	—
l	457	49	37	58	86	—	—	—
m	461	49	35	49	83	19	22	—
n	450	59	44	64	92	—	31	28
o	454	56	41	57	89	35	—	—
p	444	64	50	71	98	—	—	42
q	437	72	57	78	106	—	—	33
r	459	50	36	56	84	—	38	—
s	439	70	56	77	104	—	—	—
t	432	79	64	81	112	70	—	—

Table 7 Calculated PA and ETE values (kJ mol^{-1}) for compounds **a–t** in methanol

	N1 (A)		N2 (A)		O1 (B)		N2 (B)		O1 (C)		O2 (C)		O3 (C)	
	PA	ETE	PA	ETE	PA	ETE	PA	ETE	PA	ETE	PA	ETE	PA	ETE
a	139	369	133	360	176	338	197	346	—	—	—	—	—	—
b	138	370	132	361	169	341	199	340	152	354	—	—	—	—
c	140	369	133	360	176	338	200	343	—	—	156	356	—	—
d	140	368	134	360	177	337	200	344	—	—	—	—	156	348
e	138	371	132	363	174	340	198	345	—	—	—	—	—	—
f	139	371	133	362	175	340	198	346	—	—	—	—	—	—
g	139	370	133	362	175	339	198	345	—	—	—	—	—	—
h	135	377	128	370	166	345	196	350	—	—	—	—	—	—
i	139	373	133	366	176	342	199	347	—	—	—	—	—	—
j	136	374	130	366	171	344	196	349	—	—	—	—	—	—
k	141	363	133	362	172	336	199	347	—	—	—	—	—	—
l	140	366	134	360	177	338	200	343	—	—	—	—	—	—
m	140	370	132	363	175	335	200	344	137	342	138	345	—	—
n	137	372	134	361	177	337	200	343	—	—	140	341	141	337
o	139	370	133	361	170	341	200	343	156	333	—	—	—	—
p	139	368	134	360	176	338	199	343	—	—	—	—	157	329
q	140	369	133	361	179	336	199	344	—	—	—	—	157	313
r	139	369	133	361	176	339	199	344	—	—	147	350	—	—
s	139	370	133	361	177	339	199	344	—	—	—	—	—	—
t	136	375	130	366	167	346	197	347	128	373	—	—	—	—

HAT route is a one-step process defined with the BDE parameter, which describes the ease of the X–H bond homolytic cleavage (X = O or N). Here, the radical species is inactivated with the direct transfer of the hydrogen atom.[68] On the other hand, in the SET-PT mechanism, the transfer of hydrogen is observed as a two-stage process. The SET-PT occurs with electron transfer from the antioxidant to the radical species, after which the radical-cationic antioxidant is formed.[65] This step is described with the value of IP since its related to the antioxidant's ability to ionise. The second step involves proton transfer from the radical-cationic antioxidant to radical species. Here, the PDE value defines this process since the dissociation of the proton is required. In the SPLET route, these two processes are observed oppositely, *i.e.*, the reaction is initiated with the deprotonation of antioxidant, while in the second step the electrons are transferred.[69] Hence, the possibility of the SPLET pathway is affected by the values of PA and ETE. All these processes could be influenced by the solvent's polarity; therefore, the calculations were performed in methanol, water, and benzene. The high values of IP indicated that the SET-PT can be eliminated as a scavenging route in all investigated solvents (Tables 5–7 and S3–S8†). In polar solvents, PA values were significantly lower than BDE, which designated the SPLET mechanism as a thermodynamically more favourable antioxidant pathway. On the other hand, in benzene as a solvent, the HAT mechanism is slightly predominant over the SPLET since the values of BDE were somewhat lower than PA. Generally, the BDEs were lower in benzene in comparison to the polar solvents, whereas PA values were higher. Such an outcome could be expected since the reactions involving charged intermediates are less likely to occur in a non-polar environment. Moreover, all parameters suggested an almost insignificant contribution of B-ring groups in antioxidant activity, especially –NH. This can be observed by the comparison of calculated parameters to other investigated positions. The most favourable involvement in antioxidant activity was noticed for C-ring positions of the most active compounds **m**, **n**, and **o**, which represents additional proof of their enhanced activity, as well as for the ring A –NH group in position 2. Also, the numbers suggested a significant influence of the ring A –NH group in position 1. All these observations pointed out ring A as most responsible for the antioxidant activity of compounds **a–t**, as well as ring C in the cases where its involvement is possible.

A more profound comprehension of the preferable radical quenching mechanism was reached by calculating the reaction enthalpies (ΔH_{BDE}, ΔH_{IP} and ΔH_{PDE}, ΔH_{PA}, and ΔH_{ETE}) for the reactions of **a–t** with the selected radicals. Here, seven radical species were chosen upon their cellular presence and behaviour ($^{\bullet}OCH_3$, $^{\bullet}OC(CH_3)_3$, $^{\bullet}OH$, $^{\bullet}OOH$, $^{\bullet}OOCH_3$, $^{\bullet}OO–CH{=}CH_2$, and $O_2^{\bullet-}$),[70] as well as DPPH. To estimate the influence of polar and non-polar surroundings, calculations were performed in different solvents (methanol, water, and benzene), and the electronic properties of selected radicals were accounted for as well.[71] The results obtained in methanol for the most active derivative **m** are presented in Table 8, while all other results are provided in the ESI (Tables S9–S65†). The obtained results varied in dependence on radical species, reaction media (solvent), and investigated analogue, but some general trends were noticed. The SET-PT mechanism can be excluded in all investigated solvents. Here, the high positive values ΔH_{IP} indicated that ionisation of **a–t** is an endothermic step with a high energy barrier, which eliminated the SET-PT as a preferable scavenging route. In benzene, energy requirements for ionisation were even higher than in polar solvents. The possibility of SET-PT could be noted for some derivatives only in the reaction with DPPH in polar solvents, where the values of ΔH_{IP} were at

Table 8 Calculated reaction enthalpies (kJ mol^{-1}) for the reactions of compound **m** with the selected radical species in methanol

m		HAT	SET-PT		SPLET	
Radical		ΔH_{BDE}	ΔH_{IP}	ΔH_{PDE}	ΔH_{PA}	ΔH_{ETE}
$^{\bullet}OCH_3$	N1 (A)	−79	84	−162	−72	−7
	N2 (A)	−93		−177	−79	−14
	N2 (B)	−45		−129	−12	−33
	O1 (B)	−79		−163	−37	−42
	O1 (C)	−109		−193	−74	−35
	O2 (C)	−106		−190	−74	−33
$^{\bullet}OC(CH_3)_3$	N1 (A)	−87	84	−171	−80	−7
	N2 (A)	−101		−185	−88	−13
	N2 (B)	−53		−137	−20	−33
	O1 (B)	−87		−171	−46	−41
	O1 (C)	−118		−202	−83	−35
	O2 (C)	−114		−199	−82	−32
$^{\bullet}OH$	N1 (A)	−150	5	−155	−64	−86
	N2 (A)	−165		−169	−72	−93
	N2 (B)	−116		−121	−4	−112
	O1 (B)	−150		−155	−30	−121
	O1 (C)	−181		−186	−67	−114
	O2 (C)	−178		−183	−66	−111
$^{\bullet}OOH$	N1 (A)	−10	106	−116	−26	16
	N2 (A)	−25		−131	−33	9
	N2 (B)	24		−83	34	−11
	O1 (B)	−11		−117	9	−19
	O1 (C)	−41		−147	−28	−13
	O2 (C)	−38		−144	−28	−10
$^{\bullet}OOCH_3$	N1 (A)	−3	115	−118	−27	24
	N2 (A)	−17		−132	−35	17
	N2 (B)	31		−84	33	−2
	O1 (B)	−3		−118	8	−11
	O1 (C)	−34		−148	−30	−4
	O2 (C)	−30		−145	−29	−1
$^{\bullet}OO–CH{=}CH_2$	N1 (A)	−2	95	−98	−7	5
	N2 (A)	−17		−112	−15	−2
	N2 (B)	31		−64	53	−22
	O1 (B)	−3		−98	28	−30
	O1 (C)	−33		−129	−10	−24
	O2 (C)	−30		−125	−9	−21
DPPH	N1 (A)	26	83	−57	33	−7
	N2 (A)	11		−72	26	−14
	N2 (B)	60		−24	93	−34
	O1 (B)	25		−58	68	−42
	O1 (C)	−5		−88	31	−36
	O2 (C)	−2		−85	31	−33
$O_2^{\bullet-}$	N1 (A)	62	273	−211	46	16
	N2 (A)	47		−225	39	9
	N2 (B)	96		−177	106	−11
	O1 (B)	62		−211	81	−19
	O1 (C)	31		−242	44	−13
	O2 (C)	34		−238	44	−10

least comparable with ΔH_{BDE} and ΔH_{PA}. In polar solvents, the competition between HAT and SPLET mechanisms was observed, although the HAT is slightly prevailing in most cases. Only in the case of $^{\bullet}OH$ radical, the HAT is clearly predominant due to higher differences between ΔH_{BDE} and ΔH_{PA}. On the other hand, in benzene as a solvent, the SPLET pathway is prevailing in all cases, except in the reactions with DPPH where the HAT mechanism is more favourable. Mutual comparison of calculated reaction enthalpies within specified positions revealed more favourable engagement of certain groups. Here, the high engagement of ring C –OH groups (analogues **m–q**) in the antioxidant activity, as well as ring A –NH groups was noted, with the low contribution of ring B groups.

Radical adduct formation (RAF) mechanism

Besides HAT, SET-PT, and SPLET antioxidant pathways, the formation of radical adduct was investigated for the reactions of compounds **a–t** with $^{\bullet}OH$ radical. In this antioxidant route, the addition of the radical species to the antioxidant occurs, resulting in the formation of the radical adduct. To determine the most favourable sites for the radical attack, the Fukui functions were calculated for all compounds.[72] Here, the values of f^{0}_{nbo} revealed multiple positions for radical attack (higher values indicate higher probability, Tables S68–S87†). Therefore, the structures of the formed radical adducts were optimised for each reaction site of each compound. The enthalpies of the reactions with $^{\bullet}OH$ radical were calculated in methanol and benzene as solvents (Tables 9 and S68–S87†). Atom labelling is provided in Tables S68–S87.†

Based on the obtained ΔH_{RAF} values in methanol, in almost all cases (except derivatives **h**, **i**, **j**, and **t**), the formation of the

Table 9 Calculated reaction enthalpies (kJ mol^{-1}) for the radical adduct formation of compounds **a–t** with $^{\bullet}OH$ radical[a]

Entry	Position	ΔH_{RAF} (methanol)	ΔH_{RAF} (benzene)
a + $^{\bullet}OH$	C20*	−90	−97
b + $^{\bullet}OH$	C19*	−89	−85
c + $^{\bullet}OH$	C20*	−89	−97
d + $^{\bullet}OH$	C20*	−90	−97
e + $^{\bullet}OH$	C19*	−89	−96
f + $^{\bullet}OH$	C20*	−90	−96
g + $^{\bullet}OH$	C20*	−90	−97
h + $^{\bullet}OH$	C9#	−40	−42
i + $^{\bullet}OH$	C10#	−102	−57
j + $^{\bullet}OH$	C10#	−100	−57
k + $^{\bullet}OH$	C19*	−88	−98
l + $^{\bullet}OH$	C20*	−90	−98
m + $^{\bullet}OH$	C19*	−87	−95
	C1	−84	−78
	C35	−84	−89
n + $^{\bullet}OH$	C22*	−90	−98
	C2	−90	−80
	C3	−88	−92
o + $^{\bullet}OH$	C18*	−88	−86
	C2	−81	−82
	C3	−88	−80
p + $^{\bullet}OH$	C20*	−91	−97
	C34	−95	−85
	C35	−84	−79
q + $^{\bullet}OH$	C33	−106	−103
	C19*	−91	−98
r + $^{\bullet}OH$	C17*	−90	−97
s + $^{\bullet}OH$	C19*	−87	−98
t + $^{\bullet}OH$	C4	−85	−77
	C32	−77	−72

[a] Symbols * and # match equivalent sites for the radical attack for all compounds.

radical adduct occurs on the pyrazolone ring A, where the carbon atom bearing methyl group (labelled with *, Table 9), was identified as the most reactive site for radical attack. Here, the influence of ring C substitution was noticed, *i.e.*, in all these cases, all analogues bear an electron-donating group on ring C. On the other hand, when the electron-withdrawing group is introduced (derivatives **h**, **i**, **j**), the highest probability for radical adduct formation is on the pyrazole B ring, on the carbon neighbouring the methine group (labelled with #, Table 9). Additionally, for derivatives **m–q**, the formation of radical adduct could occur on ring C, initiated with the radical attack on carbon atoms bearing hydroxy or methoxy groups. Such an outcome could be linked to the proximity of oxygen atoms and their involvement in the stabilisation of the formed radical adduct.[73] Similarly, in the case of **t**, the most reactive sites were identified on ring C, particularly on the C32, which is between two carbon atoms substituted with chlorine. An analogous trend was observed in benzene as a solvent.

Comparing the values of ΔH_{RAF} obtained in methanol (Table 9) with ΔH_{BDE} values obtained for the reactions with $^{\bullet}$OH radical (Tables 8 and S9–S27†), it could be observed that the HAT pathway is still predominant since ΔH_{RAF} is significantly higher than ΔH_{BDE}. On the other hand, in comparison to ΔH_{IP} and ΔH_{PDE}, ΔH_{PA}, and ΔH_{ETE} values, the RAF mechanism is prevailing over SET-PT and SPLET in polar solvents.

Conclusions

In this work, the antioxidant potency of the selected pyrazolone derivatives **a–t** was assessed using *in vitro* and *in silico* methods. The obtained results revealed great radical scavenging abilities of the investigated compounds against the DPPH radical (IC_{50} values in the range of 2.6–7.8 μM). All compounds expressed higher antioxidant potency than the parent pyrazolone compound. The results indicated the dependence of the substituents on ring C, *i.e.*, on their number, position, and nature. In comparison to the non-substituted analogue, enhanced antioxidant activity was noted for derivatives bearing R^2-substituent on the ring C (compounds **c** (R^2–OH), **e** (R^2–Cl), **i** (R^2–NO_2), and **l** (R^2–CH_3)). Furthermore, the enhancement was even more noticeable in the cases of compounds **m** and **n** bearing catechol moiety, which exhibited the best antioxidant activity (IC_{50} = 2.6 and 2.9 μM, respectively). On the other hand, R^1-substitution was generally identified as the least favourable for radical scavenging, especially when the electron-withdrawal group is introduced. Density functional theory calculations were in good agreement with experimental results. From the thermodynamical point of view, the calculated descriptors indicated compounds **m**, **n**, and **o** within the most prominent ones. The prediction of the most preferable antioxidant pathway was performed in the absence and presence of radical species, as well as in polar and non-polar surroundings. In the absence of free radicals, in polar solvents, the SPLET mechanism is a favourable scavenging route, whereas in nonpolar the HAT is slightly predominant. In the presence of radical species, the obtained values of the reaction enthalpies revealed that HAT is slightly prevailing in polar solvents, while the SPLET is prevalent in nonpolar. Additionally, the radical adduct formation (RAF) pathway was investigated with $^{\bullet}$OH radical. The obtained results revealed that RAF prevails over SPLET in polar solvents, whereas HAT is preferable radical scavenging pathway than RAF, and that the formation of the radical adduct is dependent on ring C substitution. The presence of electron-donating groups favours radical adduct formation on the pyrazolone ring A, while the electron-withdrawing group induce radical adduct formation on the pyrazole B ring. In the cases where ring C bears hydroxy or methoxy groups, the formation of radical adduct could occur on this ring. These findings represent valuable data for this pyrazolone class and could be used as the basis for further investigations.

Experimental section

Antioxidant activity of compounds a–t

The insight into the antioxidant potency of pyrazolones **a–t** was reached using the 2,2-diphenyl-1-picrylhydrazyl (DPPH) method.[74] The samples were prepared by mixing the methanolic solution of DPPH radical (0.05 mM, 1 mL) with the tested compound (20 μL of different concentrations in dimethyl sulfoxide (DMSO) and 980 μL of methanol). After the incubation period (twenty and sixty minutes in a dark room at room temperature), the absorbance was determined spectrophotometrically at 517 nm. Quercetin and nordihydroguaiaretic acid were used as reference compounds, whereas methanol was a control solution. All measurements were made in triplicate. The IC_{50} values (which represent a minimal concentration of the assessed compound necessary for 50% of a maximum scavenging capacity) were determined for all compounds (regression equations are given in Table S88†) and presented as mean values ± standard deviation (SD) of three independent measurements. For all compounds, the stoichiometric factor (SF) was calculated using the equation:[75,76]

$$SF = [DPPH]/(2\times IC_{50}) \quad (1)$$

Density functional theory (DFT) calculations

The density functional theory (DFT) method was used for the calculation of equilibrium geometries of pyrazolones **a–t** (**Pyr**) and all radical species, employing the Gaussian 09 program package.[77] All calculations were performed using the B3LYP/6-311+g(d,p) level of theory.[78–80] The SMD solvation model was applied for the calculations in different solvents (methanol, water, and benzene).[81] Methanol was chosen since it was used in the *in vitro* experiments. Calculations were made in water to mimic the polar environment of the living cell, as well as in benzene to simulate nonpolar surroundings. Depending on the molecule state, charges and multiplicities were properly assigned to each species (for neutral molecules charge = 0/multiplicity = 1; for anions charge = −1/multiplicity = 1; for radicals charge = 0/multiplicity = 2; and for radical cations charge = 1/multiplicity = 2). Unrestricted spin calculations were performed for open-shell systems. Thermodynamic parameters required for the estimation of the preferable radical scavenging mechanism, *i.e.*, bond dissociation enthalpy (BDE), ionisation potential (IP), proton affinity (PA), proton

dissociation enthalpy (PDE), and electron transfer enthalpy (ETE) were calculated using the eqn (2)–(6):

$$\mathrm{BDE} = H(\mathbf{Pyr}^{\bullet}) + H(\mathrm{H}^{\bullet}) - H(\mathbf{Pyr}) \quad (2)$$

$$\mathrm{IP} = H(\mathbf{Pyr}^{\bullet+}) + H(\mathrm{e}^{-}) - H(\mathbf{Pyr}) \quad (3)$$

$$\mathrm{PDE} = H(\mathbf{Pyr}^{\bullet}) + H(\mathrm{H}^{+}) - H(\mathbf{Pyr}^{\bullet+}) \quad (4)$$

$$\mathrm{PA} = H(\mathbf{Pyr}^{-}) + H(\mathrm{H}^{+}) - H(\mathbf{Pyr}) \quad (5)$$

$$\mathrm{ETE} = H(\mathbf{Pyr}^{\bullet}) + H(\mathrm{e}^{-}) - H(\mathbf{Pyr}^{-}) \quad (6)$$

For the estimation of the preferred antiradical pathway in the presence of selected radical species, reaction enthalpies defined with eqn (7)–(12) were calculated at 298 K.[82] The values of the solvation enthalpies of electron and proton were acquired from the literature.[83] Stabilisation energies (ΔE_{iso}) were calculated to evaluate the radical stability at a particular position following the eqn (13),[82] whereas the reaction enthalpies for the formation of radical adducts were acquired using the eqn (14):

$$\Delta_{\mathrm{r}}H_{\mathrm{BDE}} = [H(\mathbf{Pyr}^{\bullet}) + H(\mathrm{R{-}OH})] - [H(\mathbf{Pyr}) + H(\mathrm{R{-}O}^{\bullet})] \quad (7)$$

$$\Delta_{\mathrm{r}}H_{\mathrm{IP}} = [H(\mathbf{Pyr}^{\bullet+}) + H(\mathrm{R{-}O}^{-})] - [H(\mathbf{Pyr}) + H(\mathrm{R{-}O}^{\bullet})] \quad (8)$$

$$\Delta_{\mathrm{r}}H_{\mathrm{PDE}} = [H(\mathbf{Pyr}^{\bullet}) + H(\mathrm{R{-}OH})] - [H(\mathbf{Pyr}^{\bullet+}) + H(\mathrm{R{-}O}^{-}) \quad (9)$$

$$\Delta_{\mathrm{r}}H_{\mathrm{PA}} = [H(\mathbf{Pyr}^{-}) + H(\mathrm{R{-}OH})] - [H(\mathbf{Pyr}) + H(\mathrm{R{-}O}^{-})] \quad (10)$$

$$\Delta_{\mathrm{r}}H_{\mathrm{ETE}} = [H(\mathbf{Pyr}^{\bullet}) + H(\mathrm{R{-}O}^{-})] - [H(\mathbf{Pyr}^{-}) + H(\mathrm{R{-}O}^{\bullet})] \quad (11)$$

$$\Delta_{\mathrm{r}}H_{\mathrm{BDE}} = \Delta_{\mathrm{r}}H_{\mathrm{IP}} + \Delta_{\mathrm{r}}H_{\mathrm{PDE}} = \Delta_{\mathrm{r}}H_{\mathrm{PA}} + \Delta_{\mathrm{r}}H_{\mathrm{ETE}} \quad (12)$$

$$\Delta E_{\mathrm{iso}} = (H(\mathbf{Pyr}^{\bullet}) + H(\mathrm{Ph{-}OH})) - (H(\mathbf{Pyr}) + H(\mathrm{Ph{-}O}^{\bullet}) \quad (13)$$

$$\Delta_{\mathrm{r}}H_{\mathrm{RAF}} = H(\mathbf{Pyr}{-}\mathrm{OH}^{\bullet}) - H(\mathbf{Pyr}) - H(^{\bullet}\mathrm{OH}) \quad (14)$$

Author contributions

Conceptualisation, V. P.; methodology, J. B., and D. S.; validation, J. B., and V. M.; formal analysis, J. B., and V. P.; investigation, J. B., and V. M.; resources, V. P., and Z. P.; data curation, J. B., and V. P.; writing—original draft preparation J. B.; writing—review and editing, V. P., D. S., and Z. P; visualisation, J. B., and V. P.; supervision, V. P.; project administration, V. P. and Z.P.; funding acquisition, V. P., and Z. P. All authors have read and agreed to the published version of the manuscript.

Conflicts of interest

There are no conflicts to declare.

Acknowledgements

This work was supported by the Serbian Ministry of Education, Science and Technological Development (Agreement No. 451-03-68/2022-14/200122, 451-03-68/2022-14/200088, and 451-03-68/2022-14/200378).

References

1 Z. Wang, in *Comprehensive Organic Name Reactions and Reagents*, John Wiley & Sons, Inc., Hoboken, NJ, USA, 2010, pp. 331–334.
2 G. Mustafa, M. Zia-ur-Rehman, S. H. Sumrra, M. Ashfaq, W. Zafar and M. Ashfaq, *J. Mol. Struct.*, 2022, **1262**, 133044.
3 A. Kadam, B. Dawane, M. Pawar, H. Shegokar, K. Patil, R. Meshram and R. Gacche, *Bioorg. Chem.*, 2014, **53**, 67–74.
4 Z. Zhao, X. Dai, C. Li, X. Wang, J. Tian, Y. Feng, J. Xie, C. Ma, Z. Nie, P. Fan, M. Qian, X. He, S. Wu, Y. Zhang and X. Zheng, *Eur. J. Med. Chem.*, 2020, **186**, 111893.
5 W. Sneader, in *Drug Discovery*, John Wiley & Sons, Ltd, Chichester, UK, 2006, pp. 115–150.
6 I. Nikolova, V. Petkova, J. Tencheva, N. Benbasat, J. Voinikov and N. Danchev, *Biotechnol. Biotechnol. Equip.*, 2013, **27**, 3605–3619.
7 S. Adhikari, M. Singh, P. Sharma and S. Arora, *J. Appl. Pharm. Sci.*, 2021, **11**, 26–37.
8 A. Indrasena, S. Riyaz, P. L. Mallipeddi, P. Padmaja, B. Sridhar and P. K. Dubey, *Tetrahedron Lett.*, 2014, **55**, 5014–5018.
9 S. Shubhalaxmi, L. Pathak, K. Ananda and K. S. Bhat, *Cogent Chem.*, 2016, **2**, 1141388.
10 R. Al-Saheb, S. Makharza, F. Al-Battah, R. Abu-El-Halawa, T. Kaimari and O. S. Abu Abed, *Biosci. Rep.*, 2020, **40**, 1–13.
11 N. Parmar, S. Teraiya, R. Patel, H. Barad, H. Jajda and V. Thakkar, *J. Saudi Chem. Soc.*, 2015, **19**, 36–41.
12 S. Shamsuzzaman, A. Mashrai, A. Ahmad, A. M. Dar, H. Khanam, M. Danishuddin and A. U. Khan, *Med. Chem. Res.*, 2014, **23**, 348–362.
13 S. K. Krishnasamy, V. Namasivayam, S. Mathew, R. S. Eakambaram, I. A. Ibrahim, A. Natarajan and S. Palaniappan, *Arch. Pharm.*, 2016, **349**, 383–397.
14 A. Dahal, M. Lo, S. Singh, H. Vo, D. ElHage, S. D. Jois and S. Murru, *Chem. Biol. Drug Des.*, 2022, **99**, 620–633.
15 K. M. Vyas, R. N. Jadeja, D. Patel, R. V. Devkar and V. K. Gupta, *Polyhedron*, 2013, **65**, 262–274.
16 R. Pettinari, F. Marchetti, C. Pettinari, A. Petrini, R. Scopelliti, C. M. Clavel and P. J. Dyson, *Inorg. Chem.*, 2014, **53**, 13105–13111.
17 N. A. Khalil, E. M. Ahmed, K. O. Mohamed, Y. M. Nissan and S. A. B. Zaitone, *Bioorg. Med. Chem.*, 2014, **22**, 2080–2089.
18 G. Mariappan, B. P. Saha, L. Sutharson, A. Singh, S. Garg, L. Pandey and D. Kumar, *Saudi Pharmaceut. J.*, 2011, **19**, 115–122.
19 M. T. El Sayed, M. A. M. S. El-Sharief, E. S. Zarie, N. M. Morsy, A. R. Elsheakh, A. Voronkov, V. Berishvili and G. S. Hassan, *Bioorg. Med. Chem. Lett.*, 2018, **28**, 952–957.
20 R. V. Antre, *Med. Chem.*, 2012, **02**, 126–130.
21 A. A. Moneer, K. O. Mohammed and H. B. El-Nassan, *Chem. Biol. Drug Des.*, 2016, **87**, 784–793.
22 C. Dohutia, P. P. Kaishap and D. Chetia, *Int. J. Pharm. Sci.*, 2013, **5**, 86–90.

23 N. Uramaru, H. Shigematsu, A. Toda, R. Eyanagi, S. Kitamura and S. Ohta, *J. Med. Chem.*, 2010, **53**, 8727–8733.
24 X. Fan, X. Zhang, L. Zhou, K. A. Keith, E. R. Kern and P. F. Torrence, *Bioorg. Med. Chem. Lett.*, 2006, **16**, 3224–3228.
25 V. A. Obakachi, N. D. Kushwaha, B. Kushwaha, M. C. Mahlalela, S. R. Shinde, I. Kehinde and R. Karpoormath, *J. Mol. Struct.*, 2021, **1241**, 130665.
26 N. Atatreh, S. Hasan, B. R. Ali and M. A. Ghattas, *Acta Pharm.*, 2021, **71**, 325–333.
27 J. E. Cadena-Cruz, L. M. Guamán-Ortiz, J. C. Romero-Benavides, N. Bailon-Moscoso, K. E. Murillo-Sotomayor, N. V. Ortiz-Guamán and J. Heredia-Moya, *BMC Chem.*, 2021, **15**, 38.
28 T. Anwar, H. Nadeem, S. Sarwar, H. Naureen, S. Ahmed, A. U. Khan and M. Arif, *Drug Dev. Res.*, 2020, **81**, 893–903.
29 E. A. Orabi, M. A. A. Orabi, M. H. Mahross and M. Abdel-Hakim, *J. Saudi Chem. Soc.*, 2018, **22**, 705–714.
30 Z. Zhang, M. Cheng, J. Guo, Y. Wan, R. Wang, Y. Fang, Y. Jin, S. S. Xie and J. Liu, *J. Mol. Struct.*, 2022, **1254**, 132319.
31 E. Çınar, E. Başaran, Ö. Erdoğan, R. Çakmak, M. Boğa and Ö. Çevik, *J. Chin. Chem. Soc.*, 2021, **68**, 2355–2367.
32 M. Messaad, I. Dhouib, M. Abdelhedi and B. Khemakhem, *J. Mol. Struct.*, 2022, **1263**, 133105.
33 S. Yousuf, K. M. Khan, U. Salar, S. Chigurupati, M. T. Muhammad, A. Wadood, M. Aldubayan, V. Vijayan, M. Riaz and S. Perveen, *Eur. J. Med. Chem.*, 2018, **159**, 47–58.
34 F. Chaudhry, S. Naureen, S. Choudhry, R. Huma, M. Ashraf, M. al-Rashida, B. Jahan, M. Hyder Khan, F. Iqbal, M. Ali Munawar and M. Ain Khan, *Bioorg. Chem.*, 2018, **77**, 507–514.
35 R. C. Kulkarni, J. M. Madar, S. L. Shastri, F. Shaikh, N. S. Naik, R. B. Chougale, L. A. Shastri, S. D. Joshi, S. R. Dixit and V. A. Sunagar, *Chem. Data Collect.*, 2018, **17–18**, 497–506.
36 V. Hadi, Y. H. Koh, T. W. Sanchez, D. Barrios, N. Neamati and K. W. Jung, *Bioorg. Med. Chem. Lett.*, 2010, **20**, 6854–6857.
37 Y. Kakiuchi, N. Sasaki, M. Satoh-Masuoka, H. Murofushi and K. Murakami-Murofushi, *Biochem. Biophys. Res. Commun.*, 2004, **320**, 1351–1358.
38 H. Ashtekar, N. Aggarwal, Z. Fernandes, A. Rao and N. Varghese, *Res. Square*, 2022.
39 C. Bailly, P. E. Hecquet, M. Kouach, X. Thuru and J. F. Goossens, *Bioorg. Med. Chem.*, 2020, **28**, 115463.
40 L. S. Zondagh, S. F. Malan and J. Joubert, *J. Enzyme Inhib. Med. Chem.*, 2020, **35**, 1596–1605.
41 S. Perrone, M. Szabó, C. V. Bellieni, M. Longini, M. Bangó, D. Kelen, A. Treszl, S. Negro, M. L. Tataranno and G. Buonocore, *Pediatr. Neurol.*, 2010, **43**, 236–240.
42 H. Yoshida, H. Yanai, Y. Namiki, K. Fukatsu-Sasaki, N. Furutani and N. Tada, *CNS Drug Rev.*, 2006, **12**, 9–20.
43 J. R. Walker, K. E. Fairfull-Smith, K. Anzai, S. Lau, P. J. White, P. J. Scammells and S. E. Bottle, *Medchemcomm*, 2011, **2**, 436–441.
44 J. Branković, V. M. Milovanović, D. Simijonović, S. Novaković, Z. D. Petrović, S. S. Trifunović, G. A. Bogdanović and V. P. Petrović, *RSC Adv.*, 2022, **12**, 16054–16070.
45 M. Zarghani and B. Akhlaghinia, *RSC Adv.*, 2015, **5**, 87769–87780.
46 J. Safaei-Ghomi, B. Khojastehbakht-Koopaei and H. Shahbazi-Alavi, *RSC Adv.*, 2014, **4**, 46106–46113.
47 J. Safaei-Ghomi, B. Khojastehbakht-Koopaei and S. Zahedi, *Chem. Heterocycl. Compd.*, 2015, **51**, 34–38.
48 A. Vafaee, A. Davoodnia and M. Pordel, *Res. Chem. Intermed.*, 2015, **41**, 8343–8354.
49 R. Ramesh, N. Nagasundaram, D. Meignanasundar, P. Vadivel and A. Lalitha, *Res. Chem. Intermed.*, 2017, **43**, 1767–1782.
50 S. Sadjadi, M. M. Heravi, V. Zadsirjan and V. Farzaneh, *Res. Chem. Intermed.*, 2018, **44**, 6765–6785.
51 Z. Zhou and Y. Zhang, *Green Chem. Lett. Rev.*, 2014, **7**, 18–23.
52 N. G. Khaligh, S. B. A. Hamid and S. J. J. Titinchi, *Chin. Chem. Lett.*, 2016, **27**, 104–108.
53 G. Mohammadi Ziarani, F. Saidian, P. Gholamzadeh, A. Badiei, J. B. Ghasemi, E. Aghaee and A. Abolhasani Soorki, *J. Iran. Chem. Soc.*, 2019, **16**, 1401–1409.
54 M. Miliovsky, I. Svinyarov, Y. Mitrev, Y. Evstatieva, D. Nikolova, M. Chochkova and M. G. Bogdanov, *Eur. J. Med. Chem.*, 2013, **66**, 185–192.
55 S. Y. Li, X. B. Wang and L. Y. Kong, *Eur. J. Med. Chem.*, 2014, **71**, 36–45.
56 A. Jain, S. Yadav and P. Malhotra, *J. Chem. Sci.*, 2021, **133**, 1–8.
57 E. S. S. Priya, R. P. Nayak, P. Saldanha, B. J. Mohan and A. Prabhu, *Int. J. Curr. Res. Rev.*, 2020, **12**(23), 68–75.
58 S. R. Kang and Y. R. Lee, *Mol. Divers.*, 2015, **19**, 293–304.
59 V. W. Barajas-Carrillo, A. Estolano-Cobián, L. Díaz-Rubio, R. R. Ayllón-Gutiérrez, R. Salazar-Aranda, R. Díaz-Molina, V. García-González, H. Almanza-Reyes, I. A. Rivero, J. G. Marrero and I. Córdova-Guerrero, *Med. Chem. Res.*, 2021, **30**, 610–623.
60 O. G. Idemudia, A. I. Okoh, A. P. Sadimenko, E. C. Hosten and O. O. Okoh, *J. Chem.*, 2017, **2017**, 1–10.
61 L. Valgimigli, R. Amorati, M. G. Fumo, G. A. DiLabio, G. F. Pedulli, K. U. Ingold and D. A. Pratt, *J. Org. Chem.*, 2008, **73**, 1830–1841.
62 A. Torres de Pinedo, P. Peñalver and J. C. Morales, *Food Chem.*, 2007, **103**, 55–61.
63 M. C. Foti, E. R. Johnson, M. R. Vinqvist, J. S. Wright, L. R. C. Barclay and K. U. Ingold, *J. Org. Chem.*, 2002, **67**, 5190–5196.
64 M. C. Foti, L. R. C. Barclay and K. U. Ingold, *J. Am. Chem. Soc.*, 2002, **124**, 12881–12888.
65 C. Y. Lee, A. Sharma, J. Semenya, C. Anamoah, K. N. Chapman and V. Barone, *Antioxidants*, 2020, **9**, 1–14.
66 S. Antonczak, *J. Mol. Struct.*, 2008, **856**, 38–45.
67 H. Zhou, X. Li, Y. Shang and K. Chen, *Antioxidants*, 2019, **8**, 590.
68 L. Capaldo and D. Ravelli, *Eur. J. Org. Chem.*, 2017, **2017**, 2056–2071.
69 I. O. Alisi, A. Uzairu and S. E. Abechi, *Bull. Natl. Res. Cent.*, 2020, **44**, 137.

70 A. Amić, Z. Marković, J. M. D. Marković, S. Jeremić, B. Lučić and D. Amić, *Comput. Biol. Chem.*, 2016, **65**, 45–53.
71 J. Xie and K. M. Schaich, *J. Agric. Food Chem.*, 2014, **62**, 4251–4260.
72 R. G. Parr and W. Yang, *Theory of Orientation and Steroselection*, Springer-Verlag, 1984, vol. 106.
73 D. A. Milenković, D. S. Dimić, E. H. Avdović, A. D. Amić, J. M. Dimitrić Marković and Z. S. Marković, *Chem. Eng. J.*, 2020, **395**, 124971.
74 C. Kontogiorgis and D. Hadjipavlou-Litina, *J. Enzyme Inhib. Med. Chem.*, 2003, **18**, 63–69.
75 D. Dimić, D. Milenković, J. Dimitrić Marković and Z. Marković, *Phys. Chem. Chem. Phys.*, 2017, **19**, 12970–12980.
76 M. C. Foti, *J. Agric. Food Chem.*, 2015, **63**, 8765–8776.
77 M. J. Frisch, G. W. Trucks, H. B. Schlegel, G. E. Scuseria, M. a. Robb, J. R. Cheeseman, G. Scalmani, V. Barone, G. a. Petersson, H. Nakatsuji, X. Li, M. Caricato, a. V. Marenich, J. Bloino, B. G. Janesko, R. Gomperts, B. Mennucci, H. P. Hratchian, J. V. Ortiz, a. F. Izmaylov, J. L. Sonnenberg, D. Williams-Young, F. Ding, F. Lipparini, F. Egidi, J. Goings, B. Peng, A. Petrone, T. Henderson, D. Ranasinghe, V. G. Zakrzewski, J. Gao, N. Rega, G. Zheng, W. Liang, M. Hada, M. Ehara, K. Toyota, R. Fukuda, J. Hasegawa, M. Ishida, T. Nakajima, Y. Honda, O. Kitao, H. Nakai, T. Vreven, K. Throssell, J. A. Montgomery Jr, J. E. Peralta, F. Ogliaro, M. J. Bearpark, J. J. Heyd, E. N. Brothers, K. N. Kudin, V. N. Staroverov, T. a. Keith, R. Kobayashi, J. Normand, K. Raghavachari, a. P. Rendell, J. C. Burant, S. S. Iyengar, J. Tomasi, M. Cossi, J. M. Millam, M. Klene, C. Adamo, R. Cammi, J. W. Ochterski, R. L. Martin, K. Morokuma, O. Farkas, J. B. Foresman and D. J. Fox, *GAUSSIAN 16 (Revision C.01)*, Gaussian Inc., Wallingford, CT, 2016.
78 C. Lee, W. Yang and R. G. Parr, *Phys. Rev. B: Condens. Matter Mater. Phys.*, 1988, **37**, 785–789.
79 A. D. Becke, *J. Chem. Phys.*, 1993, **98**, 5648–5652.
80 T. H. Dunning, *J. Chem. Phys.*, 1989, **90**, 1007–1023.
81 A. V. Marenich, C. J. Cramer and D. G. Truhlar, *J. Phys. Chem. B*, 2009, **113**, 4538–4543.
82 Z. D. Petrović, J. Orović, D. Simijonović, V. P. Petrović and Z. Marković, *RSC Adv.*, 2015, **5**, 24094–24100.
83 Z. Marković, J. Tošović, D. Milenković and S. Marković, *Comput. Theor. Chem.*, 2016, **1077**, 11–17.